Transport in Porous Media (2022) 145:1–12
https://doi.org/10.1007/s11242-021-01735-7

Percolativity of Porous Media

R. Hilfer[1] **· J. Hauskrecht**[1]

Received: 19 April 2021 / Accepted: 13 December 2021 / Published online: 29 August 2022

Abstract
Connectivity and connectedness are nonadditive geometric functionals on the set of pore scale structures. They determine transport of mass, volume or momentum in porous media, because without connectivity there cannot be transport. Percolativity of porous media is introduced here as a geometric descriptor of connectivity, that can be computed from the pore scale and persists to the macroscale through a suitable upscaling limit. It is a measure that combines local percolation probabilities with a probability density of ratios of eigenvalues of the tensor of local percolating directions. Percolativity enters directly into generalized effective medium approximations. Predictions from these generalized effective medium approximations are found to be compatible with apparently anisotropic Archie correlations observed in experiment.

Keywords Connectivity · Percolation · Upscaling · Local porosity theory · Porous media · Pore scale transport · Pore scale geometry · Anisotropy · Geometric characterization

1 Introduction

Advances of a fundamental nature in theories of transport in porous media rely on upscaling microstructural information from the pore scale to larger-scale models (Blunt 2017; Keller and Holzer 2017; Samouelian et al. 2007). Despite experimental and computational progress predictive upscaling is often hampered by a lack of microstructural foundations or clear pore scale concepts for quantities related to the connectivity of porous media.

Many attempts to characterize connectivity, e.g., the concept of percolation probability as an order parameter for connectedness (Essam 1980, Fig. 7) (Ohser et al. 2012), originate from percolation theory (Broadbent and Hammersley 1957; Stauffer and Aharony 1992). Another example from percolation theory is the pair-connectedness function (Essam 1980; Stauffer and Aharony 1992). In Hilfer (1991) local percolation probabilities were introduced to combine concepts from percolation theory with ideas from finite size scaling theory (Binder 1992; Hilfer 1994) resulting in a successful explanation of Archies's law (Archie 1942) for the resistivity of porous media. Other suggestions include n-connectedness (Ohser and Schladitz 2009) or the Euler characteristic (Schlüter and Vogel 2011; Chiu

✉ R. Hilfer
hilfer@icp.uni-stuttgart.de

[1] Universität Stuttgart, Allmandring 3, 70569 Stuttgart, Deutschland

et al. 2013; Jiang and Arns 2020). Recently (Berg 2012; Hauskrecht 2018; Slotte et al. 2020), tortuosity (Krüger 1918; Scheidegger 1957; Bear 1972) and constrictivity (Owen 1952; Boyack and Giddings 1963) have found some attention. Except for nonintersecting capillaries however, the latter quantities cannot be computed from the geometry alone (Ghanbarian et al. 2012; Hauskrecht 2018). More specifically, they require the solution of a physical boundary value problem.

Due to experimental difficulty and lack of theoretical concepts the connectivity of porous media has remained one of the key sources of uncertainty. Extending pore scale concepts such as local percolation probabilities (Biswal et al. 1999; Keller et al. 2013) is thus of paramount importance. In this conceptual work we introduce percolativity as an upscaled quantity related to local percolation probability.

Geometric characterization of connectivity requires a definition of porous media as a starting point. Let us emphasize that in this paper, contrary to common practice, we do not define porous media as realizations of random sets (Chiu et al. 2013). Our starting point is rather a given and fixed sufficiently large (ideally infinite) pore space $\mathbb{p} \subset \mathbb{R}^3$. Regarding porous media as random sets requires one to specify their probability distribution. In applications this distribution is usually not known. Accordingly, in this paper upscaling proceeds by volume averaging (Whitaker 1999) instead of averaging over an unknown distribution of pore scale geometries (Chiu et al. 2013). Macroscopic quantities emerge as limits of sequences of volume averaged microscopic functions.

2 Objective and Problem Statement

The objective of this work is to upscale the local percolation probabilities of local porosity theory from the pore scale to the Darcy scale. To state the problem more clearly recall the definition of local percolation probabilities (Hilfer 1991, 2002).

Let $\mathcal{K}$ denote the set of all compact and convex subsets of $\mathbb{R}^3$ and let $\mathcal{R}$ be the set of countable unions of sets from $\mathcal{K}$. Heterogeneous or porous samples $\mathbb{S} = \mathbb{p} \cup \mathbb{m} \subset \mathbb{R}^3$ are assumed to consist of a pore space $\mathbb{p} \in \mathcal{R}$ and a matrix space $\mathbb{m} \in \mathcal{R}$, each of which belong to the convex ring $\mathcal{R}$. Let $\mathbb{K} \in \mathcal{K}$ be a convex and compact set with centroid at the origin $0 \in \mathbb{R}^3$. Then

$$\mathbb{K}(\mathbf{r}) = \mathbf{r} + \mathbb{K} = \{\mathbf{r} + \mathbf{q} \in \mathbb{R}^3 : \mathbf{q} \in \mathbb{K}\} \tag{1}$$

denotes its translate by a vector $\mathbf{r} \in \mathbb{R}^3$. If the measurement cell $\mathbb{K} = \mathbb{K}(0, \ell) = \{(x, y, z) \in \mathbb{R}^3 : |x| \le \ell/2, |y| \le \ell/2, |z| \le \ell/2\}$ is a cube of sidelength ℓ, then its boundary

$$\partial\mathbb{K} = \partial\mathbb{K}_x^+ \cup \partial\mathbb{K}_x^- \cup \partial\mathbb{K}_y^+ \cup \partial\mathbb{K}_y^- \cup \partial\mathbb{K}_z^+ \cup \partial\mathbb{K}_z^- \tag{2}$$

may be decomposed into its six faces, where $\partial\mathbb{K}_\alpha^\pm$ denotes the pair of opposite faces perpendicular to the α-direction ($\alpha = x, y, z$). In (Biswal et al. 1998; Hilfer 2002) such a measurement cell $\mathbb{K}(\mathbf{r}, \ell)$ was called percolating in the α-direction (with $\alpha = x, y, z$) if there exists a continuous path

$$\begin{aligned} \mathbf{p} : [0, 1] &\to \mathbb{R}^3 \\ t &\mapsto \mathbf{p}(t) = \mathbf{p}_t \end{aligned} \tag{3}$$

with

$$\mathbf{p}_0 \in \mathbb{p} \cap \partial \mathbb{K}_\alpha^-(\mathbf{r}, \ell) \tag{4a}$$

$$\mathbf{p}_t \in \mathbb{p} \cap \mathbb{K}(\mathbf{r}, \ell) \qquad \text{for all } t \in [0,1], \tag{4b}$$

$$\mathbf{p}_1 \in \mathbb{p} \cap \partial \mathbb{K}_\alpha^+(\mathbf{r}, \ell). \tag{4c}$$

Three basic local percolation indicators were defined in (Biswal et al. 1998; Hilfer 2002) as

$$\Lambda_\alpha(\mathbf{r}, \ell) = \begin{cases} 1 & \text{if } \mathbb{K}(\mathbf{r}, \ell) \text{ is percolating} \\ 0 & \text{otherwise} \end{cases} \tag{5a}$$

for $\alpha = x, y, z$, and two additional ones

$$\Lambda_3(\mathbf{r}, \ell) = \Lambda_x(\mathbf{r}, \ell)\Lambda_y(\mathbf{r}, \ell)\Lambda_z(\mathbf{r}, \ell) \tag{5b}$$

$$\Lambda_c(\mathbf{r}, \ell) = \operatorname{sgn}(\Lambda_x(\mathbf{r}, \ell) + \Lambda_y(\mathbf{r}, \ell) + \Lambda_z(\mathbf{r}, \ell)) \tag{5c}$$

indicate percolation in all three directions (Λ_3), resp. in at least one direction (Λ_c). The local percolation probabilities are defined as

$$\lambda_\alpha(\phi;\ell) = \frac{\sum_{\mathbf{r}} \Lambda_\alpha(\mathbf{r}, \ell)\delta_{\phi,\phi(\mathbf{r},\ell)}}{\sum_{\mathbf{r}} \delta_{\phi,\phi(\mathbf{r},\ell)}} \tag{6}$$

where the summation runs over all centroids (i.e., placements) of measurement cells,

$$\phi(\mathbf{r}, \ell) = \frac{|\mathbb{p} \cap \mathbb{K}(\mathbf{r}, \ell)|}{|\mathbb{K}(\mathbf{r}, \ell)|} \tag{7}$$

is the local porosity in the measurement cell $\mathbb{K}(\mathbf{r}, \ell)$, and

$$\delta_{\phi,\phi(\mathbf{r},\ell)} = \begin{cases} 0 & \text{if } \phi = \phi(\mathbf{r}, \ell) \\ 1 & \text{otherwise} \end{cases} \tag{8}$$

the Kronecker symbol. The local percolation probabilities give the fraction of measurement cells of sidelength ℓ with local porosity ϕ that percolate in the α-direction, where $\alpha = x, y, z, 3, c$.

Three problems arise from this definition. Firstly, the local percolation probability λ_α depends on the size and shape of the measurement cell $\mathbb{K}$. This problem arises also for the local porosity distributions. Secondly there are five scalar quantities λ_α. Their definition seems to depend on the ability to identify "opposite" boundaries of a measurement cell $\mathbb{K}$. And thirdly the local percolation probabilities are not tensorial, although transport coefficients are in general tensors.

3 Method

The problems will be approached using the method of weak scaling limits from Hilfer (2018). The method of weak limits is based on mathematical theorems arising in the problem of finding minimizers of nonlinear functionals formulated as integrals over

infinite dimensional spaces (Ball 1989). It was successfully used in Hilfer (2018, Sec. VI) for local porosity distributions.

For local percolation probabilities the method of weak scaling limits becomes applicable upon a modification of the percolation criterion in Eq. (4). A measurement cell $\mathbb{K}(\mathbf{r}) = \mathbf{r} + \mathbb{K}$ is now called *percolating*, if there exists a continuous path as in Eq. (3) with

$$\mathbf{p}_0 \in \mathbb{p} \cap \partial\mathbb{K}(\mathbf{r}) \tag{9a}$$

$$\mathbf{p}_t \in \mathbb{p} \cap \mathbb{K}(\mathbf{r}) \qquad \text{for all } t \in [0,1], \tag{9b}$$

$$\mathbf{p}_1 \in \mathbb{p} \cap \left\{\partial\mathbb{K}(\mathbf{r}) \setminus \mathbb{B}\big(\mathbf{p}_0, |\mathbf{r}-\mathbf{p}_0|\big)\right\} \tag{9c}$$

where $\mathbb{B}(\mathbf{x}, a) = \{\mathbf{r} \in \mathbb{R}^3 \,:\, |\mathbf{r}-\mathbf{x}| \le a\}$ denotes a ball of radius a centered at $\mathbf{x}$. This percolation criterion is illustrated in Fig. 1. The dashed path is percolating, while the dash-dotted path is not. The new criterion (9) applies equally to spherical, ellipsoidal or other convex measurement cells.

Let $\mathbb{R}^3 = \mathbb{p} \cup \mathbb{m}$ be a sufficiently large (ideally infinite) microstructure at the pore scale consisting of a pore space $\mathbb{p}$ and matrix $\mathbb{m}$ being its complement. A Darcy scale porous medium $\overline{\mathbb{S}}$ with this pore scale substructure is represented as the cartesian product $\overline{\mathbb{S}} \times \mathbb{R}^3$. At each macropoint $\overline{\mathbf{r}} \in \overline{\mathbb{S}}$ the set $\{\overline{\mathbf{r}}\} \times \mathbb{R}^3$ represents the pore scale substructure with pore space $\mathbb{p}$ and matrix $\mathbb{m}$ such that $\mathbb{R}^3 = \mathbb{p} \cup \mathbb{m}$. The dimensionless position vectors at the pore scale, denoted as $\mathbf{r} \in \mathbb{R}^3$, and the Darcy scale, denoted as $\overline{\mathbf{r}} \in \overline{\mathbb{S}}$, are related as $\mathbf{r} = a\overline{\mathbf{r}}$ by a scale separation factor $a \gg 1$ (ideally $a \to \infty$). Let $1 \le a_i < \infty$ be a sequence of scale separation factors diverging to infinity, $a_i \to \infty$ as $i \to \infty$, and let $\mathbf{r}_i \in \mathbb{R}^3$ be a sequence of points such that $|\mathbf{r}_i| \le \sqrt{a_i}$. The sequence of mappings ($i \in \mathbb{N}$)

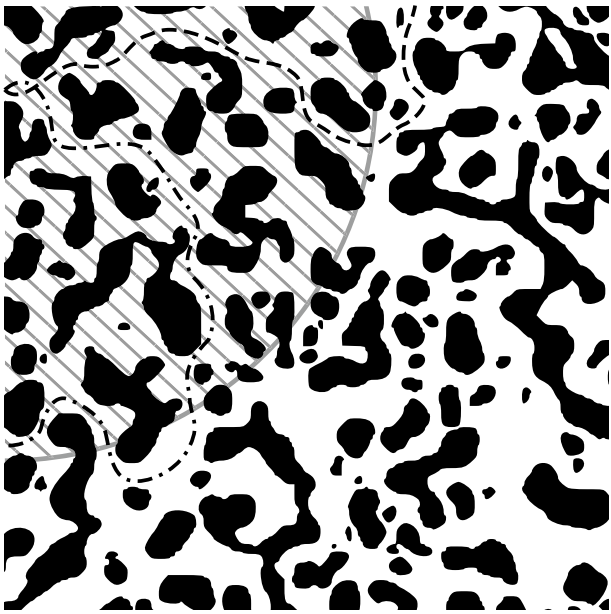

Fig. 1 Two paths starting at $\mathbf{p}_0$ on the left boundary. The grey hatched circle centered at $\mathbf{p}_0$ represents the forbidden ball $\mathbb{B}\big(\mathbf{p}_0, |\mathbf{r}-\mathbf{p}_0|\big)$. The dashed path is percolating according to percolation criterion (9) while the dash-dotted path is non-percolating. Both paths are non-percolating in the x-, y- or z-direction according to (4)

$$\begin{aligned} \sigma_i : \overline{\mathbb{S}} &\to \overline{\mathbb{S}} \times \mathbb{R}^3 \\ \overline{\mathbf{r}} &\mapsto (\overline{\mathbf{r}}, \mathbf{r}_i + a_i \overline{\mathbf{r}}) \end{aligned} \tag{10}$$

is now used for upscaling geometric quantities from the pore scale to the Darcy scale. Here and in the following $\overline{\mathbf{r}} \in \overline{\mathbb{S}}$ is always assumed to be an interior point of $\overline{\mathbb{S}}$, i.e., not on its boundary.

Let $g : \mathbb{R}^3 \to \mathbb{G} \subset \mathbb{R}^m$ be the bounded and non-random geometric quantity that is to be upscaled to the Darcy scale. Its values fall into the bounded set $\mathbb{G} \subset \mathbb{R}^m$. They represent m pore scale geometric parameters such as porosity. To every g is associated a function $g^\times : \overline{\mathbb{S}} \times \mathbb{R}^3 \to \overline{\mathbb{S}} \times \mathbb{G}$ that maps $(\overline{\mathbf{r}}, \mathbf{r}) \mapsto (\overline{\mathbf{r}}, g(\mathbf{r}))$. Then the sequence σ_i gives rise to a sequence $G(\,\cdot\,;i) = \pi \circ g^\times \circ \sigma_i$ of Darcy scale functions ($i \in \mathbb{N}$)

$$\begin{aligned} G(\,\cdot\,;i) : \overline{\mathbb{S}} \xrightarrow{\sigma_i} \quad & \overline{\mathbb{S}} \times \mathbb{R}^3 \quad \xrightarrow{g^\times} \quad \overline{\mathbb{S}} \times \mathbb{G} \quad \xrightarrow{\pi} \quad \mathbb{G} \\ \overline{\mathbf{r}} \mapsto \quad & (\overline{\mathbf{r}}, \mathbf{r}_i + a_i \overline{\mathbf{r}}) \quad \mapsto (\overline{\mathbf{r}}, g(a_i \overline{\mathbf{r}} + \mathbf{r}_i)) \quad \mapsto g(a_i \overline{\mathbf{r}} + \mathbf{r}_i) =: G(\overline{\mathbf{r}};i) \end{aligned} \tag{11}$$

where π is the projection onto the second component. Note, that the sequence $G(\,\cdot\,;i)$ need not converge. Let $\overline{\mathbb{K}}(\overline{\mathbf{r}})$ denote a Darcy scale measurement cell centered at $\overline{\mathbf{r}} \in \overline{\mathbb{S}}$ on the Darcy scale, and let $0 < b_i \leq 1$ be a sequence of shrinkage factors with $b_i \xrightarrow{i\to\infty} 0$. If the sequence $G(\,\cdot\,;i)$ is uniformly bounded, and if $\mathbb{A} \subset \mathbb{G}$ is measurable, then the limit

$$\mu_{\overline{\mathbf{r}}}(\mathbb{A}) = \lim_{i\to\infty} \frac{\left| \left\{ \overline{\mathbf{s}} \in b_i\, \overline{\mathbb{K}}(\overline{\mathbf{r}}) \,:\, G(\overline{\mathbf{s}};i) \in \mathbb{A} \right\} \right|}{\left| b_i\, \overline{\mathbb{K}}(\overline{\mathbf{r}}) \right|} \tag{12}$$

exists (Hilfer 2018, Theorem 3). The number $0 \leq \mu_{\overline{\mathbf{r}}}(\mathbb{A}) \leq 1$ gives the probability to find the values $(G_1, ..., G_m) \in \mathbb{A}$ for the m geometrical quantities on the Darcy scale. The family of measures $\mu_{\overline{\mathbf{r}}}$ parameterized by $\overline{\mathbf{r}}$ is a family of probability measures whenever $\mu_{\overline{\mathbf{r}}}(\mathbb{G}) = 1$ for all $\overline{\mathbf{r}}$ in the interior of $\overline{\mathbb{S}}$.

4 Results

4.1 Local Connectivity

This section applies Eq. (12) to connectivity. The geometric quantities $g : \mathbb{R}^3 \to \mathbb{G}$ in the previous section are specified here as $g = (\Lambda, d, e)$ and $\mathbb{G} = \{0\} \cup (\{1\} \times [0,1] \times [0,1])$. To define the three geometric quantities Λ, d and e that will be used to characterize local anisotropic connectivity in a clear way, local percolation clusters and local percolating directions need to be introduced first.

Local percolating clusters $\mathbb{p}_i^p \subset \mathbb{K}(\mathbf{r}) \cap \mathbb{p}$, $i \in \mathbb{N}$ are defined as connectedness components containing a percolating path in the sense of Eq. (9). The superscript p stands for

"percolating". The total number of percolating clusters in $\mathbb{K}(\mathbf{r})$ is denoted as $n_{\mathbb{p}}(\mathbb{K}(\mathbf{r}))$. The set of *local percolating directions* for a measurement cell $\mathbb{K}(\mathbf{r})$ centered at $\mathbf{r}$ is defined as

$$\mathbb{L}(\mathbb{K}(\mathbf{r})) = \left\{ \frac{\mathbf{q}-\mathbf{r}}{|\mathbf{q}-\mathbf{r}|} \in \mathbb{S}^2 : \mathbf{q} \in \bigcup_{i=1}^{n_{\mathbb{p}}(\mathbb{K}(\mathbf{r}))} \mathbb{p}_i^p \cap \partial\mathbb{K}(\mathbf{r}) \right\} \tag{13}$$

where $\mathbb{S}^2 = \partial\mathbb{B}(\mathbf{0}, 1)$ is the unit sphere.

With these preparations the first geometric quantity Λ, called the *local percolation indicator*, is defined as

$$\Lambda(\mathbb{K}(\mathbf{r})) = \begin{cases} 0 & \text{if } \mathbb{L}(\mathbb{K}(\mathbf{r})) = \emptyset \\ 1 & \text{otherwise} \end{cases} \tag{14}$$

using the set $\mathbb{L}(\mathbb{K}(\mathbf{r}))$ of local percolating directions. In other words, it is defined to be 0 for non-percolating cells and 1 for percolating cells.

To define the remaining two geometric quantities d, e let $\mathbf{X}(\mathbf{r}) = \mathbf{r} \otimes \mathbf{r}$ denote the simple tensor obtained as the tensor product of $\mathbf{r}$ with itself. The set $\mathbb{L}$ of local percolating directions then defines a tensor

$$\mathbf{I}_{\mathbb{p}}(\mathbb{K}(\mathbf{r})) = \frac{1}{4\pi} \int_{\mathbb{L}(\mathbb{K}(\mathbf{r}))} \mathbf{X}(\mathbf{q}) \mathrm{d}^2\mathbf{q} \tag{15a}$$

obtained for every cell by integration over its (two-dimensional) set of local percolating directions. It is normalized as

$$\mathbf{J}_{\mathbb{p}}(\mathbb{K}(\mathbf{r})) = \frac{\mathbf{I}_{\mathbb{p}}(\mathbb{K}(\mathbf{r}))}{\mathrm{Tr}\, \mathbf{I}_{\mathbb{p}}(\mathbb{K}(\mathbf{r}))} \tag{15b}$$

by dividing with the trace. The non-negative eigenvalues $J_{\mathbb{p}a}(\mathbb{K}(\mathbf{r}))$, $J_{\mathbb{p}b}(\mathbb{K}(\mathbf{r}))$, $J_{\mathbb{p}c}(\mathbb{K}(\mathbf{r}))$ obey $J_{\mathbb{p}a}(\mathbb{K}(\mathbf{r})) + J_{\mathbb{p}b}(\mathbb{K}(\mathbf{r})) + J_{\mathbb{p}c}(\mathbb{K}(\mathbf{r})) = 1$, and are assumed to be ordered as $1 \geq J_{\mathbb{p}a} \geq J_{\mathbb{p}b} \geq J_{\mathbb{p}c} \geq 0$. Then the remaining two local connectivity characteristics are defined as the ratios

$$d = \frac{J_{\mathbb{p}b}}{J_{\mathbb{p}a}}, \qquad e = \frac{J_{\mathbb{p}c}}{J_{\mathbb{p}b}} \tag{16}$$

of these eigenvalues. By definition they fall into the unit interval. When $\Lambda = 0$ the set $\mathbb{L}$ is empty and hence d, e do not exist. This concludes the definition of the three geometric quantities $g = (\Lambda, d, e)$.

To illustrate the generality and flexibility of the three geometric quantities $g = (\Lambda, d, e)$ for the characterization of local connectivity it is pointed out, that meaningful modifications are possible by modifying the definition of the set of local percolating directions. An alternative definition is

$$\mathbb{L}(\mathbb{K}(\mathbf{r})) = \left\{ \frac{\mathbf{p}_0 - \mathbf{p}_1}{|\mathbf{p}_0 - \mathbf{p}_1|} \in \mathbb{S}^2 : \mathbf{p}_0, \mathbf{p}_1 \in \partial\mathbb{K}(\mathbf{r}), \mathbf{p}_0 \rightsquigarrow \mathbf{p}_1 \right\} \tag{17}$$

where $\mathbf{p}_0 \rightsquigarrow \mathbf{p}_1$ means that $\mathbf{p}_0$ is the starting point and $\mathbf{p}_1$ is the end point of a percolation path in the sense of Eq. (9). Experimental observations or numerical calculations of the

sets $\mathbb{L}(\mathbb{K}(\mathbf{r}))$ must answer the question whether Eqs. (13) or (17) is better suited to characterize anisotropic connectivity of porous media.

The family of probability measures $\mu_{\overline{\mathbf{r}}}$ parametrized by the macropoint $\overline{\mathbf{r}}$ can be used to characterize local connectivity. The local percolation probability function is defined as the conditional probability $\mu_{\overline{\mathbf{r}}}(\{\Lambda = 1\}|\{d = d_{\mathbb{p}}, e = e_{\mathbb{p}}\})$ that a measurement cell is percolating given the condition that the local anisotropy parameters have the values $d = d_{\mathbb{p}}, e = e_{\mathbb{p}}$. One finds

$$\lambda_{\overline{\mathbf{r}}}(d_{\mathbb{p}}, e_{\mathbb{p}}) = \mu_{\overline{\mathbf{r}}}(\{\Lambda = 1\}|\{d = d_{\mathbb{p}}, e = e_{\mathbb{p}}\}) = \begin{cases} 1 & d_{\mathbb{p}}, e_{\mathbb{p}} \in \mathrm{supp}(\mu_{\overline{\mathbf{r}}}) \\ 0 & \text{otherwise,} \end{cases} \tag{18}$$

because the local anisotropy parameters are defined only for cells with $\Lambda = 1$ and thus $\mu_{\overline{\mathbf{r}}}(\{d = d_{\mathbb{p}}, e = e_{\mathbb{p}}\})$ equals $\mu_{\overline{\mathbf{r}}}(\{\Lambda = 1, d = d_{\mathbb{p}}, e = e_{\mathbb{p}}\})$. The total percolation probability

$$\begin{aligned} p_{\overline{\mathbf{r}}} &= \int_0^1 \int_0^1 \lambda_{\overline{\mathbf{r}}}(d_{\mathbb{p}}, e_{\mathbb{p}}) \mu_{\overline{\mathbf{r}}}(1, d_{\mathbb{p}}, e_{\mathbb{p}}) \mathrm{d}e_{\mathbb{p}} \mathrm{d}d_{\mathbb{p}} = \int_0^1 \int_0^1 \mu_{\overline{\mathbf{r}}}(1, d_{\mathbb{p}}, e_{\mathbb{p}}) \mathrm{d}e_{\mathbb{p}} \mathrm{d}d_{\mathbb{p}} \\ &= \int_{\mathbb{G}} \mathrm{d}\mu_{\overline{\mathbf{r}}}(\Lambda = 1, d, e) = \mu_{\overline{\mathbf{r}}}(\{1\} \times [0,1] \times [0,1]) = 1 - \mu_{\overline{\mathbf{r}}}(\{\Lambda = 0\}) \end{aligned} \tag{19}$$

is independent of the anisotropy parameters. Both quantities, $p_{\overline{\mathbf{r}}}$ and $\lambda_{\overline{\mathbf{r}}}(d_{\mathbb{p}}, e_{\mathbb{p}})$, characterize connectivity at the Darcy scale.

4.2 Percolativity

Applying Eq. (12) to a uniformly bounded but not necessarily convergent sequence of functions $G(\,\cdot\,;i)$ yields a measure $\mu_{\overline{\mathbf{r}}}$ parametrized by $\overline{\mathbf{r}} \in \overline{\mathbb{S}}$ with the following property. If $A : \mathbb{G} \to \mathbb{R}$ is any continuous function of the pore scale connectivity characterized by g, then

$$\lim_{i\to\infty} \int_{\overline{\mathbb{S}}} A[g(\overline{\mathbf{r}};i)] f(\overline{\mathbf{r}}) \mathrm{d}\overline{\mathbf{r}} = \int_{\overline{\mathbb{S}}} f(\overline{\mathbf{r}}) \int_{\mathbb{G}} A(G) \mathrm{d}\mu_{\overline{\mathbf{r}}}(G)\, \mathrm{d}\overline{\mathbf{r}} = \int_{\overline{\mathbb{S}}} f(\overline{\mathbf{r}}) \overline{A}(\overline{\mathbf{r}}) \mathrm{d}\overline{\mathbf{r}} \tag{20}$$

for all integrable functions $f : \overline{\mathbb{S}} \to \mathbb{R}$. Here the notation

$$\overline{A}(\overline{\mathbf{r}}) := \int_{\mathbb{G}} A(G) \mathrm{d}\mu_{\overline{\mathbf{r}}}(G) \tag{21}$$

was introduced. In other words the measure $\mu_{\overline{\mathbf{r}}}(G)$ can be used to compute Darcy scale expectation values of any continuous function of pore scale connectivity or connectedness. In this sense the measure $\mu_{\overline{\mathbf{r}}}(G)$ characterizes connectivity on the Darcy scale. For this reason it is given a new name, and called *percolativity*.

Four types of percolativity can arise in porous media. Percolativity of porous media can be homogeneous and non-random, if $\mathrm{d}\mu_{\overline{\mathbf{r}}}(G) = \delta(G - \overline{G})$ for all $\overline{\mathbf{r}}$, where $\overline{G}$ is a fixed macroscopic parameter. It is homogeneous and random if $\mathrm{d}\mu_{\overline{\mathbf{r}}}(G) = \mathrm{d}\mu(G)$ independent of $\overline{\mathbf{r}}$. Percolativity is heterogeneous and non-random if $\mathrm{d}\mu_{\overline{\mathbf{r}}}(G) = \delta(G - \overline{G}(\overline{\mathbf{r}}))$ where $\overline{G}(\overline{\mathbf{r}})$ is a given function. In all other cases it is heterogeneous and random.

4.3 Cylindrical Effective Medium Approximation

The new concept of percolativity can be applied straightforwardly in local porosity theory (Hilfer 1991) for resistivities, conductivities, permeabilities or other transport parameters of disordered systems. Details have been presented elsewhere (Hauskrecht 2021). Because local porosity theory is a generalized effective medium approximation of Bruggeman type (Bruggeman 1935; Landauer 1978) this application leads directly to new effective medium approximations.

Recall the classical effective medium formula for the formation factor of a homogeneous and isotropic medium with porosity $\overline{\phi}$ in the case of infinite conductivity contrast $\sigma'_{\mathbb{m}}/\sigma'_{\mathbb{p}} = 0$. Here the pore space $\mathbb{p}$ of the medium is assumed to be filled with a liquid of dc-conductivity $0 < \sigma'_{\mathbb{p}} < \infty$, the matrix is assumed to have vanishing dc-conductivity $\sigma'_{\mathbb{m}} = 0$. The formation factor $F = \sigma'_{\mathbb{p}}/\overline{\sigma}'$ is the ratio of the pore space dc-conductivity to the effective dc-conductivity $\overline{\sigma}'$ of the medium. The Bruggemann formula reads $F = 2/(3\overline{\phi} - 1)$ for $\overline{\phi} > 1/3$ and $F = \infty$ for $\overline{\phi} \le 1/3$ (Bruggeman 1935; Landauer 1978) and it exhibits a percolation singularity at $\overline{\phi} = 1/3$. This formula for isotropic media was generalized to anisotropic media where $\mathbb{p}$ is a homogeneous mixture of aligned oblate ellipsoids $(x/a)^2 + (y/b)^2 + (z/c)^2 \le 1$ with half axes $a = b \ge c$ (Schwartz 1994). In this case the formation factor F is a tensor whose eigenvalues F_x, F_y, F_z obey $F_x = F_y$, $\overline{\phi}(F_x - 1)/[1 + N_a(F_x - 1)] = (1 - \overline{\phi})/(1 - N_a)$ and $\overline{\phi}(F_z - 1)/[1 + N_c(F_z - 1)] = (1 - \overline{\phi})/(1 - N_c)$ where $1 = 2N_a + N_c$, $R = [F_x b^2/(F_z c^2) - 1]^{1/2}$, and $N_c = R^{-3}(1 + R^2)(1 - \arctan R)$ [Schwartz 1994, Eq. (8)]. These coupled equations exhibit again a percolation singularity at $\overline{\phi} = 1/3$.

To illustrate the applicability of the percolativity concept as an upscaled local percolation probability consider a constant local percolation probability function $\lambda(\overline{\mathbf{r}}) = \overline{\phi}^{1/3}$ as in the central pore model from Hilfer (1991, eq.(6.12)). More discussion of the theoretical background of this function as well as other types of functions can be found in Hilfer (1991, Sec.VI.C.2). Experimental measurements of λ were given, e.g., in Biswal et al. (1998). For general d and e the formation factor tensor is very complicated, but when $d \approx 0$ and $e \approx 1$ it simplifies considerably (Hauskrecht 2021). The special case $d \approx 0$ and $e \approx 1$ is called cylindrical, because an ellipsoid with these axis ratios degenerates into a cylinder with circular cross section. In this "cylindrical" case the formation factor tensor has eigenvalues (Hilfer and Hauskrecht 2022)

$$F_x = \begin{cases} \dfrac{1}{\overline{\phi}^{4/3}} & \text{for } \frac{1}{8} \le \overline{\phi} \le 1 \\ \dfrac{2\overline{\phi}^{1/3}}{3\overline{\phi}^{4/3} - \overline{\phi}} & \text{for } \frac{1}{27} \le \overline{\phi} \le \frac{1}{8} \\ \infty & \text{for } 0 \le \overline{\phi} \le \frac{1}{27} \end{cases} \tag{22a}$$

$$F_y = F_z = \begin{cases} \dfrac{2 - \overline{\phi}}{2\overline{\phi}^{4/3} - \overline{\phi}} & \text{for } \frac{1}{8} \le \overline{\phi} \le 1 \\ \infty & \text{for } 0 \le \overline{\phi} \le \frac{1}{8} \end{cases} \tag{22b}$$

in the x-, y- and z-direction. Note, that now the percolation singularity is anisotropic in the sense that there appear two percolation thresholds, one at $\overline{\phi} = 1/27$ for F_x and another at $\overline{\phi} = 1/8$ for $F_y = F_z$, at which the effective resistivity becomes infinite.

4.4 Anisotropic Archie Correlations

The cylindrical effective medium approximation (22) above resembles certain empirical correlations between formation factor and porosity in electrical resistivity logs observed by Archie (1942). For a detailed discussion of Archie's law within local porosity theory the reader is referred to Hilfer (1991, Sec.V.D.). Recently it has been suggested in Table 1 of Nguyen et al. (2015) that the formation factors reported by Waxman and Smits (1968) and Hill and Milburn (1956) are anisotropic and normal-to-transversal ratios as large as 5 have been reported for that data set. If their suggestions hold, and if the anisotropy of shaly sands is oblate, then a percolativity based on oblate effective medium approximation might be expected to be applicable to the experimental measurement.

Such an application is shown in Fig. 2. The negative logarithm of formation factors for several shaly sands from Table 1 in Waxman and Smits (1968) are plotted as squares and those from Table 3 in Waxman and Smits (1968) as circles against the porosities. Note that Waxman and Smits excluded the effect of surface conduction. The percolativity-based

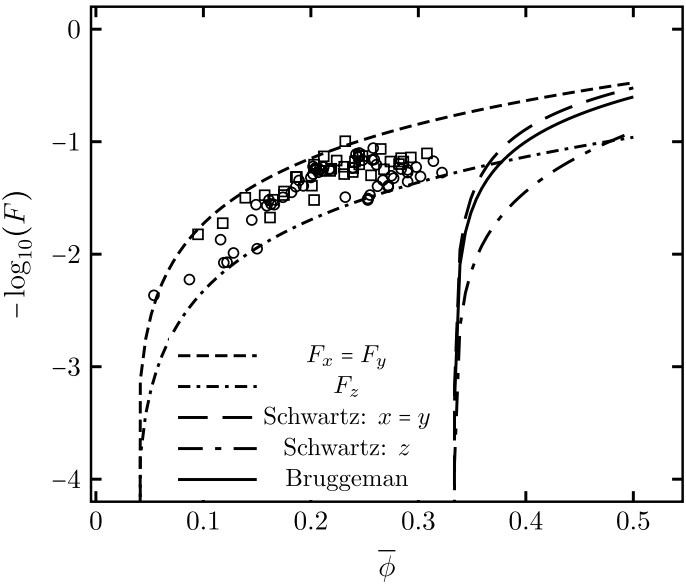

Fig. 2 Influence of percolativity on effective medium predictions for the normalized electrical resistivity (formation factor) F of anisotropic shaly sands as a function of porosity $\overline{\phi}$. The experimental data are from Table 1 (squares) and Table 3 (circles) in Waxman and Smits (1968) (see pages 110-112 in this reference for a detailed description of the samples). The two curves bounding the data points are solutions of a generalized effective medium approximation based on anisotropic percolativity with $d = 1$ and $e = 0.45$. The short-dashed upper bound is $F_x = F_y$ and the short-dash-dotted lower bound is F_z. The three curves on the right are the Bruggeman effective medium theory and its anisotropic generalization to aligned oblate ellipsoids. The isotropic Bruggeman (1935) theory with $F_x = F_y = F_z$ is shown as the solid line. The generalized anisotropic effective medium approximation from Schwartz [1994, eq.(8)] for aligned oblate ellipsoids with $d = 1$ and $e = 0.45$ is shown as the long-dashed line for $F_x = F_y$ and the long-dash-dotted line for F_z

effective medium approximation for oblate anisotropy with $d = 1$ and $e = 0.45$ is shown as a short-dashed curve for $F_x = F_y$ and a short-dash-dotted curve for F_z. As before, a constant local percolation probability function $\lambda(\overline{\mathbf{r}}) = \overline{\phi}^{1/3}$ was used. For comparison the isotropic Bruggeman (1935) effective medium equation is shown as the solid line. The percolation threshold at $\overline{\phi} = 1/3$ is clearly incompatible with the experimental data. The same holds for the generalized anisotropic effective medium approximation from Schwartz (1994). The long-dashed curve and the long-dash-dotted curves with percolation threshold at $\overline{\phi} = 1/3$ in Fig. 2 were computed using the equations in the previous section for aligned oblate ellipsoids with the same half-axis ratios $d = 1$ and $e = 0.45$. If the suggestion from Nguyen et al. (2015) holds true, that the sandy shale samples are indeed anisotropic, and if it is assumed the sample orientations are uniformly distributed, then the experimental data are seen to be compatible with a percolation threshold at $\overline{\phi} = 1/27$ as predicted by applying local porosity theory [Eq. (22)] with anisotropic percolativity.

5 Conclusion

Three problems were enunciated in Sect. 2: Firstly, the dependence of local percolation probabilities on the size and shape of measurement cells. Secondly, the dependence of local percolation probabilities on the identification of "opposite" boundaries. And thirdly, the problem that connectivity in anisotropic media might reasonably be expected to be a tensorial quantity, but local percolation probabilities are scalar, not tensorial, quantities. Two of these problems have been solved by introducing the general geometric concept of percolativity.

The first problem is solved, because the quantity $\mu_{\overline{\mathbf{r}}}$, known as a Young measure, is independent of the shape or form of the measurement cell $\overline{\mathbb{K}}(\overline{\mathbf{r}})$. The second problem is solved, because the percolation criterion introduced here requires a path to enter "sufficiently deeply into the arbitrarily shaped cell" and exit on a boundary point that is "sufficiently far away" from its entry. Percolation no longer requires exit from the "opposite" boundary and hence it no longer requires the identification of "opposite" boundaries.

Concerning the third problem, the local percolation probabilities remain scalar quantities in this work. However, the new concept of percolativity does capture the tensorial character of transport in anisotropic media. Percolativity is related with a tensor of local percolating directions. Two definitions were given to illustrate the flexibility and generality of the concept.

The concept of percolativity is a general and purely geometric concept. Percolativity can be determined for a given porous medium without solving a specific physical transport problem. It is therefore expected to be important for all forms (i.e., electrical, hydrodynamical, mechanical, chemical, etc.) of physical transport.

Application of the percolativity concept in effective medium theories gives anisotropic percolation thresholds for anisotropic porous media. Assuming that shaly sands have anisotropic formation factors suggests that percolativity might be a useful concept to explain the experimental scatter of Archie correlations quantitatively, and to deduce anisotropy parameters by inversion. We emphasize, however, that the objective of this work has not been to model the anisotropic connectivity of specific examples. Instead, this work introduces the concept of percolativity and illustrates its applicability by demonstrating its consistency with well known experimental data.

In summary, the general and purely geometric concept of percolativity, introduced here, combines local percolation probabilities with a probability density of ratios of eigenvalues

of the tensor of local percolating directions. Experiments are encouraged to further explore which of two suggested alternatives is more suitable for realistic media, and the degree to which percolativity as a directly observable measure of connectivity is a useful concept.

Funding Open Access funding enabled and organized by Projekt DEAL.

References

Archie, G.: The electrical resistivity log as an aid in determining some reservoir characteristics. Trans. AIME **146**, 54 (1942)
Ball, J.: A version of the fundamental theorem for Young measures. In: Rascle, M., Serre, D., Slemrod, M. (eds.) Partial Differential Equations and Continuum Models for Phase Transitions, Lecture Notes in Physics, vol. 344, pp. 207–215. Springer, Berlin (1989)
Bear, J.: Dynamics of Fluids in Porous Media. Elsevier, New York (1972)
Berg, C.: Re-examining Archie's law: conductance description by tortuosity and constriction. Phys. Rev. E **86**, 046314 (2012)
Binder, K.: Finite size effects at phase transitions. In: Gauster, C.H. (ed.) Computional Methods in Field Theory, p. 59. Springer, Berlin (1992)
Biswal, B., Manwart, C., Hilfer, R.: Threedimensional local porosity analysis of porous media. Phys. A **255**, 221 (1998)
Biswal, B., Manwart, C., Hilfer, R., Bakke, S., Øren, P.: Quantitative analysis of experimental and synthetic microstructures for sedimentary rock. Phys. A **273**, 452 (1999)
Blunt, M.: Multiphase Flow in Permeable Media. Cambridge University Press, Cambridge (2017)
Boyack, J., Giddings, J.: Theory of electrophoretic mobility in stabilized media. Arch. Biochem. Biophys. **100**, 16–25 (1963)
Broadbent, S., Hammersley, J.: Percolation processes I. Crystals and mazes. Math. Proc. Camb. Philos. Soc. **53**, 629 (1957)
Bruggeman, D.: Berechnung verschiedener physikalischer Konstanten von heterogenen Substanzen. Ann. Phys., 5. Folge **24**, 636 (1935)
Chiu, S., Stoyan, D., Kendall, W., Mecke, J.: Stochastic Geometry and its Applications. Wiley, Chichester (2013)
Essam, J.: Percolation theory. Rep. Prog. Phys. **43**, 835 (1980)
Ghanbarian, B., Hunt, A., Ewing, R., Sahimi, M.: Tortuosity in porous media: A critical review. Soil Sci. Soc. Am. J. **77**, 1461–1471 (2012)
Hauskrecht, J.: Untersuchungen zur Konstriktivität von Transportpfaden in porösen Medien. B.Sc Thesis, Universität Stuttgart (2018)
Hauskrecht, J.: Verallgemeinerungen der lokalen Porositätstheorie für Transporteigenschaften poröser Medien. M.Sc Thesis, Universität Stuttgart (2021)
Hilfer, R.: Geometric and dielectric characterization of porous media. Phys. Rev. B **44**, 60 (1991)
Hilfer, R.: Absence of hyperscaling violations for phase transitions with positive specific heat exponent. Z. Phys. B: Condensed Matter **96**, 63 (1994)
Hilfer, R.: Review on scale dependent characterization of the microstructure of porous media. Transp. Porous Media **46**, 373 (2002)
Hilfer, R.: Multiscale local porosity theory, weak limits, and dielectric response in composite and porous media. J. Math. Phys. **59**, 103511 (2018)
Hilfer, R., Hauskrecht, J.: Effective transport coefficients of anisotropic disordered materials. Eur. Phys. J. B. (2022)

Hill, H., Milburn, J.: Effect of clay and water salinity on electrochemical behaviour of reservoir rocks. AIME Pet. Trans. **207**, 65–72 (1956)
Jiang, H., Arns, C.: A pore-scale upscaling approach for laminated sandstones using Minkowski maps and hydraulic attributes. Water Resour. Res. **56**, e2020WR027978 (2020)
Keller, L., Holzer, L.: Image-based upscaling of permeability in Opalinus clay. J. Geophys. Res.: Solid Earth **123**, 285–295 (2017)
Keller, L., Holzer, L., Schuetz, P., Gasser, P.: Pore space relevant for gas permeability in Opalinus clay: Statistical analysis of homogeneity, percolation, and representative volume element. J. Geophys. Res. Solid Earth **118**, 2799–2812 (2013)
Krüger, E.: Die Grundwasserbewegung. Int. Mitt. Bodenkd. **8**, 105 (1918)
Landauer, R.: Electrical conductivity in inhomogeneous media. In: Garland, J., Tanner, D. (eds.) Electrical Transport and Optical Properties of Inhomogeneous Media, p. 2. American Institute of Physics, New York (1978)
Nguyen, S., Vu, M., Vu, M.: Extended analytical approach for electrical anisotropy of geomaterials. J. Appl. Geophys. **123**, 211–217 (2015)
Ohser, J., Ferrero, C., Wirjadi, O., Kuznetsova, A., Düll, J., Rack, A.: Estimation of the probability of finite percolation in porous microstructures from tomographic images. Int. J. Mat. Res. (formerly Z. Metallkd.) **103**, 184–191 (2012)
Ohser, J., Schladitz, K.: 3D Images of Materials Structures. Wiley, Weinheim (2009)
Owen, J.: The resistivity of a fluid-filled porous body. AIME Pet. Trans. **195**, 169–174 (1952)
Samouelian, A., Vogel, H., Ippisch, O.: Upscaling hydraulic conductivity based on the topology of the subscale structure. Adv. Water Resour. **30**, 1179–1189 (2007)
Scheidegger, A.: The Physics of Flow Through Porous Media. University of Toronto Press, Canada (1957)
Schlüter, S., Vogel, H.: On the reconstruction of structural and functional properties in random heterogeneous media. Adv. Water Resour. **34**, 314–325 (2011)
Schwartz, L.: Effective medium theory of electrical conduction in two component anisotropic composites. Phys. A **207**, 131 (1994)
Slotte, P., Berg, C., Khanamiri, H.: Predicting resistivity and permeability of porous media using Minkowski functionals. Transp. Porous Media **131**, 705–722 (2020)
Stauffer, D., Aharony, A.: Introduction to Percolation Theory. Taylor and Francis, London (1992)
Waxman, M., Smits, L.: Electrical conductivity in oil-bearing shaly sands. SPE J. **8**, 107–122 (1968)
Whitaker, S.: The Method of Volume Averaging. Springer, Dordrecht (1999)